Applied Surface Science 707 (2025) 163599

Contents lists available at ScienceDirect

Applied Surface Science

journal homepage: www.elsevier.com/locate/apsusc

Full Length Article

Elucidating the composition and formation mechanism of slippery films from block copolymers on doped diamond-like carbon surfaces

Takeru Omiya [a,b,c,*], Enrico Pedretti [d], Albano Cavaleiro [a,c], Rachel Gouttebaron [e], Alexandre Felten [e], Arménio C. Serra [b], Jorge F.J. Coelho [b,c], Maria Clelia Righi [d,**], Fábio Ferreira [a,c]

[a] University of Coimbra, CEMMPRE, ARISE, Department of Mechanical Engineering, Rua Luís Reis Santos, 3030-788 Coimbra, Portugal
[b] University of Coimbra, CEMMPRE, ARISE, Department of Chemical Engineering, Rua Silvio Lima, 3030-790 Coimbra, Portugal
[c] Laboratory for Wear, Testing & Materials, Instituto Pedro Nunes, Rua Pedro Nunes, 3030-199 Coimbra, Portugal
[d] Department of Physics and Astronomy, University of Bologna, Bologna 40127, Italy
[e] Synthesis, irradiation & analysis of materials (SIAM) technological platform, University of Namur, Rue de Bruxelles 61, Namur 5000, Belgium

ARTICLE INFO

Keywords:
Tribofilm formation
Block copolymers
DLC doping
Friction reduction

ABSTRACT

Silicon-doped diamond-like carbon (Si-DLC) coatings combined with nitrogen-containing block copolymers offer a promising avenue for advanced boundary lubrication. In this study, we investigate the tribological behavior of Si-DLC in the presence of poly(lauryl methacrylate)-block-poly(2-dimethylaminoethyl methacrylate) (PLMA-*b*-PDMAEMA) to elucidate the formation and stability of tribofilms. Experimental analyses using X-ray photoelectron spectroscopy (XPS) and time-of-flight secondary ion mass spectrometry (ToF-SIMS) reveal that the polymer strongly adsorbs onto Si-DLC surfaces via robust N–Si bonds. Ab initio simulations further confirm that these N–Si linkages endure sliding and load with minimal bond breakage or polymer fragmentation. Importantly, the tribofilm's formation is driven primarily by polymer adsorption and compression, rather than by tribochemical reactions. This adsorption-driven pathway results in significant friction reduction and enhanced wear resistance, highlighting the critical role of silicon doping in promoting strong interfacial anchoring of the functionalized polymer. The findings establish that PLMA-*b*-PDMAEMA acts as both a lubricant film former and a protective barrier, paving the way for new strategies to optimize boundary lubrication under harsh conditions. Overall, this study demonstrates how the synergy between functionalized polymers and doped DLC coatings can be harnessed to achieve superior tribological performance, thereby broadening the applicability of polymer-based lubrication solutions across diverse mechanical systems.

1. Introduction

Polymer lubricants have been used for many years to improve the friction-reducing and anti-wear properties of automotive engine oils and industrial lubricants [1,2]. In particular, the beneficial properties of polymer friction modifiers (PFMs) in commercial engine oils were extensively studied in the 1990 s, with their effects being attributed primarily to the local increase in viscosity due to the surface enrichment of polymer species [3–6]. One example that shows friction-reducing effects is the adsorption of polymers with amine groups on surfaces, forming lubricating films [7–10]. For example, Fan et al. showed that functionalized copolymers with amine groups form thick films on metal surfaces that significantly reduce friction [11]. In addition, Gmür et al. confirmed in studies using a Quartz Crystal Microbalance with Dissipation (QCM-D) that functionalized polymers adsorb on iron oxide-coated QCM crystals, forming thin polymer brush films [12,13]. These previous studies have shown the friction-reducing effect of functionalized copolymers by surface adsorption on steel.

However, previous studies on functionalized copolymers have primarily focused on the evaluation of steel surfaces, while diamond-like carbon (DLC) coatings have hardly been investigated, despite their high hardness and excellent wear resistance which make them widely used in the automotive industry. Recent studies using organic friction modifiers such as glycerol monooleate and glycerol have shown

* Corresponding author at: University of Coimbra, CEMMPRE, ARISE, Department of Mechanical Engineering, Rua Luís Reis Santos, 3030-788 Coimbra, Portugal.
** Corresponding author.
E-mail addresses: takeru.omiya@student.dem.uc.pt (T. Omiya), clelia.righi@unibo.it (M.C. Righi).

https://doi.org/10.1016/j.apsusc.2025.163599
Received 21 March 2025; Received in revised form 9 May 2025; Accepted 21 May 2025
Available online 22 May 2025
0169-4332/© 2025 The Authors. Published by Elsevier B.V. This is an open access article under the CC BY license (http://creativecommons.org/licenses/by/4.0/).

Table 1
Properties of pure-DLC coating and Si-DLC coatings.

DLC Name	Si [at. %]	Roughness: R_a [nm]	Hardness [GPa]	Young Modulus [GPa]	sp^3 content [%]
Pure DLC	0	4.9 ± 0.1	15.6 ± 0.6	167 ± 3	26
Si-DLC	14.4	5.2 ± 0.2	19.4 ± 0.6	204 ± 4	56

interactions on DLC surfaces and demonstrated friction-reducing effects [14,15]. Recently, significant progress has been made in the development of lubrication systems combining silicon-doped DLC (Si-DLC) films with functionalized materials, leading to macroscale superlubricity. For example, Yi et al. demonstrated that the incorporation of graphene oxide nanosheets or alkyl-functionalized black phosphorus nanosheets into lubricants can significantly reduce the friction coefficient on Si-DLC surfaces by forming robust tribofilms [16,17]. These studies highlight the effectiveness of functionalized two-dimensional materials in enhancing the lubricating performance of Si-DLC coatings. However, research on the interactions between functionalized copolymers as lubricant additives and DLC surfaces is still limited. Recently, Omiya et al. showed that doping DLC coatings with silicon (Si) promotes the adsorption of 2-dimethylaminoethyl methacrylate (DMAEMA), a well-known monomer, forming tribofilms [18]. In this study, silicon-doped DLC coatings exhibited significant friction-reducing effects and wear resistance through the interaction with DMAEMA, with N-Si bonds initiating tribofilm formation. Previous research has provided valuable insights into polymer adsorption and interactions with steel and DLC surfaces [11,18]. However, further elucidation of the mechanisms behind tribofilm formation is necessary to fully understand and optimize their lubricating performance.

This study aims to analyze the chemical composition of tribofilms using XPS and ToF-SIMS to understand the friction-reducing effects and the improvement of wear resistance of functionalized copolymers. In addition, ab initio calculations were carried out to gain atomistic insights into the complex adsorption processes of the functional group on the amorphous Si-DLC surface, with the aim of clarifying the mechanisms of lubricant film formation. This research is expected to contribute to further performance improvement of the novel lubrication system combining functionalized copolymers with doped DLC, ultimately leading to the development of higher-performance lubrication systems.

Table 2
Physical properties of synthesized polymers.

Polymer Name	PDMAEMA amount [mol%]	M_w [kg/mol]	M_w/M_n
PLMA	0	38	1.07
PLMA-*b*-PDMAEMA	5	38	1.08

2. Materials and methods

2.1. Coatings

The DLC coatings were deposited on M2 steel disks (50 mm diameter, 801 Vickers hardness), referring to previous studies [19]. The steel samples, polished to a surface roughness (Ra) of ~ 100 nm, underwent deposition in a Teer Coatings unbalanced magnetron sputtering system. This system employed four targets: pure chromium, pure graphite (two targets), and pure silicon. A 300 nm chromium interlayer was deposited first to enhance adhesion. For the Si-DLC layer, the power on graphite targets remained constant, while the silicon content was varied by adjusting the power on the silicon target. All DLC coatings were approximately 1 μm thick. The coating composition was evaluated using scanning electron microscopy equipped with energy-dispersive X-ray spectroscopy, and hardness and Young's modulus were measured using a Micromaterials Nanotest platform with a Berkovich indenter, applying a maximum load of 10 mN. Surface morphology was analyzed by AFM (Innova Veeco) in tapping mode with specific scan settings. The sp^3 content of the DLC film was evaluated based on the full width at half maximum (FWHM) of the G peak obtained from Raman spectroscopy. Properties of the coatings are summarized in Table 1, demonstrating trends in roughness, hardness, Young's modulus, and sp^3 content with varying Si content.

2.2. Lubricants

Lauryl methacrylate (LMA) and 2-dimethylaminoethyl methacrylate (DMAEMA) copolymers were prepared using Supplemental Activator and Reducing Agent Atom Transfer Radical Polymerisation (SARA ATRP) following a described procedure (Fig. 1) [10]. In brief, a Schlenk reactor was charged with copper wire and copper (II) bromide under nitrogen. Separately, a mixture of ethyl-α-bromophenyl acetate, LMA, *N,N,N,N,N*-pentamethyldiethylenetriamine, and anisole was prepared and purged with nitrogen. The reactor was then placed in a preheated oil bath to allow the polymerization of LMA to proceed for 3 h. The DMAEMA was then added for the synthesis of PLMA-*b*-PDMAEMA, and the reaction continued for another hour. To assess the tribological impact of the functional group, PLMA and PLMA-*b*-PDMAEMA were synthesized, and the DMAEMA content was determined by ^1H NMR

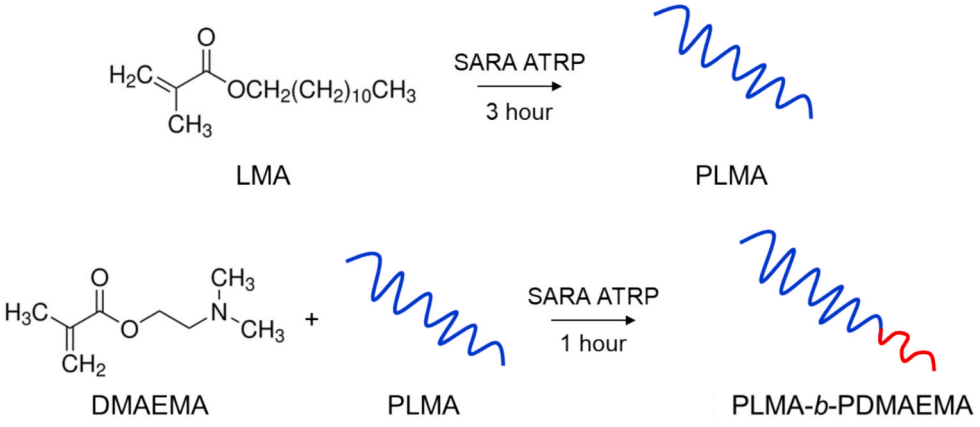

Fig. 1. Schematic diagram of PLMA and PLMA-*b*-PDMAEMA synthesized by SARA ATRP.

Table 3
Details of the tribological testing stages.

Step	1	2	3	4	5	6	7	8	9
Hz	5.00	4.50	4.00	3.50	3.00	2.75	2.50	2.25	2.0
m/s	0.150	0.135	0.120	0.105	0.090	0.083	0.075	0.068	0.060
Step	10	11	12	13	14	15	16	17	–
Hz	1.8	1.5	1.3	1.0	0.8	0.6	0.4	0.2	–
m/s	0.053	0.045	0.038	0.030	0.024	0.018	0.012	0.006	–

(Table 2). Molecular weight and dispersity were determined by multi-detectors calibration.

The polyalphaolefin 4 (PAO 4) as the base lubricant with 8 wt% of the prepared polymers was prepared by mixing 8 g of the polymer in 92 g of PAO 4 using an analytical balance. The kinematic viscosity of the solution in the presence of 8 wt% of each polymer at 80 °C was 8.5 mm^2/s.

2.3. Tribological tests

Tribological experiments were conducted using a ball-on-disk tribometer (Rtec MFT-5000) operating in reciprocating motion. A normal load of 3 N was applied, resulting in a maximum Hertzian contact pressure of 1.0 GPa. The tribometer's load cell, with a resolution of 6 mN and a maximum normal force capacity of 200 N, was calibrated by Rtec Instruments prior to testing. The tests were performed at temperatures of 80 °C, a condition known from previous studies on functionalized polymers to contribute to friction reduction [5,7]. The frequency of reciprocation varied from 5.0 to 0.2 Hz, with a stroke length of 15 mm. Each experiment was repeated three times to ensure reproducibility. Based on the Hamrock-Dowson equation, the lubrication regime was determined, with calculated λ values between 0.3 and 0.03, indicating a transition between mixed and boundary lubrication [20].

A fresh SiC ball (3/8-inch diameter, Ra 25 nm) was used for each test. Each friction test lasted 20 s, with different sliding speeds corresponding to the applied frequencies, as detailed in Table 3. The steady-state coefficient of friction (CoF) was recorded at each sliding speed. After testing, the samples were thoroughly cleaned with heptane, and their surfaces were analyzed to assess wear and lubrication effects.

2.4. Surface analysis

Surface analysis of the wear tracks was carried out using XPS and ToF-SIMS to characterize the tribofilms. XPS measurements were performed with a K-alpha XPS spectrometer (Thermo Scientific™) to investigate the surface composition. A monochromatic Al-Kα X-ray source (1468.6 eV) was used for excitation, with a spot size of 200 μm and a pass energy of 150 eV for narrow scan spectra. The binding energy scale was calibrated using the C 1 s peak at 284.8 eV as a reference. For each sample, XPS spectra were obtained from both the wear track and the unworn region to compare surface chemistry.

Additionally, the Si-DLC coating surface was analyzed using a ToF-SIMS IV (ION-TOF, Münster, Germany) equipped with a bismuth (Bi) liquid–metal ion gun at 25 keV. The ToF-SIMS spectra were recorded by scanning a Bi_3^+ ion beam over a 400 × 400 μm^2 area in an ultra-high vacuum (~10^{-7} Pa). The beam was set to bunched mode for high mass resolution, and both negative and positive spectra were obtained. The mass resolution of the secondary-ion spectra was typically around 7000. Depth profiles were performed using Cs^+ ions of 500 eV in non-interlaced mode with an analysis area of 200 × 200 μm^2. Data was acquired in negative polarity, with a flood gun used to prevent sample surface charging. Spectra processing was done using SurfaceLab 7.2 software.

2.5. Computational method

Ab initio density functional theory (DFT) [21] calculations were performed to shed light into the atomistic processes that lead to the formation of a tribofilm when combining the additive functionalization and the DLC doping by Si atoms. Since the first step necessary for the formation of a lubricating film is represented by the additive adsorption, we studied considered molecular adsorption on the amorphous Si-DLC surface. Due to the random nature of the amorphous DLC, it is of fundamental importance to study the adsorption processes from a statistical point of view. Our previous calculations on the surface of crystalline diamond have shown that DMAEMA chemisorbs on the Si-doped C(001) surface through the formation of a strong N-Si chemical bond by the functional group. Even though we tested the generalizability of this

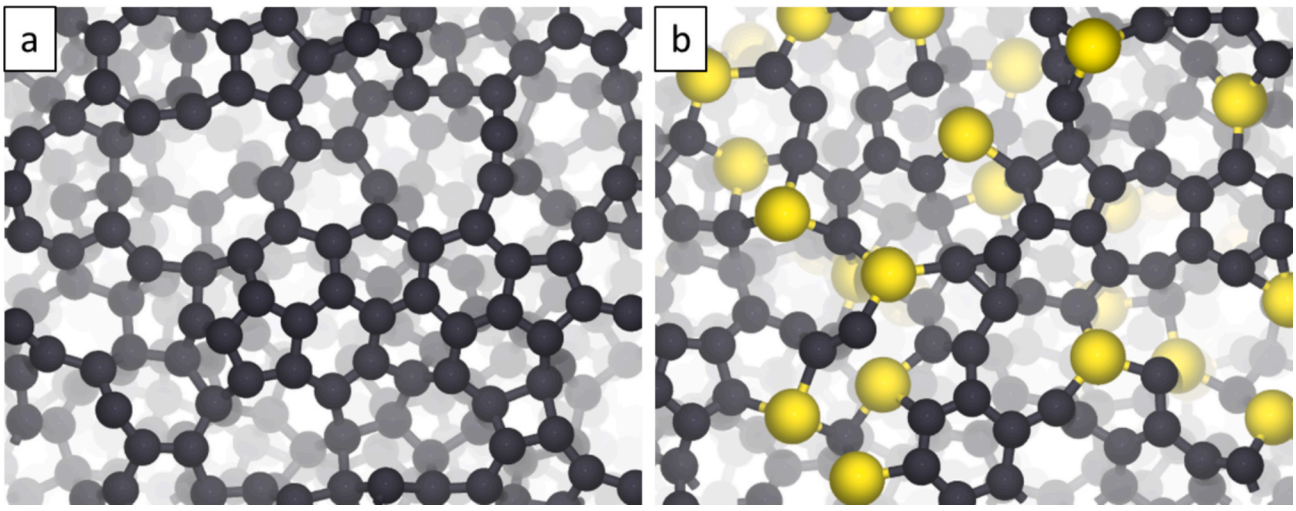

Fig. 2. undoped (a) and Si-doped (b) DLC surfaces generated with the melt-quench method for the adsorption study. Both surfaces exhibit a wide range of local environments, from graphitized regions to more reactive areas with dangling bonds.

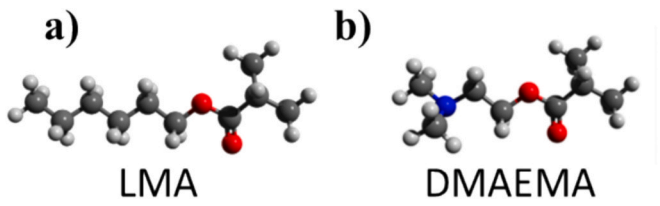

Fig. 3. Structure of the shortened LMA (a) and DMAEMA (b).

result to amorphous DLC, we considered only the adsorption of the molecule on a single substitutional Si atom within a pure DLC surface. In this work, we instead performed the full molecular adsorption study on an amorphous Si-DLC model with 10 at.% Si concentration and on an undoped DLC model. The amorphous structures were generated with melt-quench molecular dynamics simulations, using the pre-trained universal machine learning force field CHGNet [22], which, unlike to more specialized machine learning potentials published for amorphous carbon, can also describe Si-doped DLC. The obtained structures were then optimized with DFT, and validated by analyzing the radial pair distribution function, bond angle distribution and coordination number. Details about the melt-quench procedure and the validation of the structures are given in the Supplementary Information. We created two amorphous models for the Si-DLC surface to improve the statistics due to the low percentage of Si atoms, and thus the lower number of different local Si environments, while only one model was used for undoped DLC. The undoped DLC surface and one of the two Si-DLC surfaces are reported in Fig. 2.

We performed an extended study of molecular adsorption with the Xsorb program [23] that we previously developed to screen a large number of initial adsorption configurations and efficiently identify the most stable ones by employing a two-step optimization process. In the first step all the initial structures are optimized with large convergence thresholds on energy and forces, in order to obtain a reasonable guess of the configurations that will reach lower energy, and then in a subset step the low-energy configurations are fully optimized with more stringent convergence thresholds (10^{-3} Ry/bohr on forces and 10^{-4} Ry on energies).

We investigated the adsorption of the two monomers of the copolymer (DMAEMA and LMA) on undoped DLC and Si-doped DLC. The structures of the LMA and DMAEMA monomers are shown in Fig. 3. For the LMA molecule, we used a shortened hydrocarbon tail with 6 carbon atoms instead of 12, as in our previous study, to reduce the computational cost, since the full-length chain would have required larger simulation cell. On Si-doped DLC, we considered the adsorption sites on the surface of the Si atoms and generated the initial adsorption structures by placing the "reactive" atoms of the monomers, namely N and O, on these sites, including 4 horizontal molecular rotations of multiples of 90° for each site. In this way, we were able to pre-optimize 140 initial adsorption configurations for DMAEAMA on Si-DLC, of which 40 were fully optimized, and 70 initial configurations for LMA, of which 20 were fully optimized. For undoped DLC, approximately the same number of configurations were calculated, but for a single amorphous model instead of two, with the more surface-exposed carbon atoms chosen as adsorption sites. In this way, we performed more than 400 ab initio partial optimizations and 120 full structural optimizations across all molecule-surface combinations.

To test the stability of the adsorption of the copolymer under tribological conditions against the effects of temperature, load and sliding, we performed Born-Oppenheimer ab initio Molecular Dynamics (AIMD) simulations. Due to high computational cost of ab initio calculations, we only considered the functional part of the copolymer with 5 DMAEMA monomers (5-DMAEMA). We positioned the polymer at the interface between a Si-DLC bottom slab and an undoped DLC top slab, which was chosen as a non-reactive countersurface. This avoids the need to create a new DLC model in a cell with a lateral size corresponding to the lattice of the crystalline SiC countersurface used in the experiment, and only the interaction of the polymer with the bottom surface can be studied.

Finally, the nature of the tribofilm was investigated to find out whether it is formed by dissociation of the functional groups and subsequent tribochemical reactions or whether it is just an adsorbed film in which the friction- and wear-reducing effect is due to hydrocarbon tails that facilitate sliding (due to viscoelasticity) and prevent cold welding at the contact surfaces (due to steric hindrance). An indication of the polymer tendency to dissociate was obtained by performing "impact" molecular dynamics simulations. In these simulations, the polymer was placed within a Si-DLC – undoped DLC interface, in the same arrangement as in the sliding simulation, but with the top DLC slab initially positioned at a much larger vertical distance of about 10 Å above the copolymer. A normal force was applied to the top slab to accelerate it downwards and create an impulsive collision where the mechanical forces on the copolymer between the two slabs are much higher than under typical sliding conditions. These extreme conditions can be representative of the local, instantaneous force fluctuations at the contact between surface asperities and allow observation of the mechanically activated dissociation patterns of the molecule.

All *ab initio* calculations were performed with the DFT package Quantum Espresso [24], of which a version modified by our group was used for sliding MD simulations. The Perdew-Burke-Ernzerhof (PBE) parametrization [25] of the generalized gradient approximation (GGA) was used for the exchange–correlation functional, including van der Waals interactions with the semi-empirical Grimme D2 [26] scheme. Spin-polarization was included to correctly describe the chemical reactions involving the breaking and formation of new bonds, and to

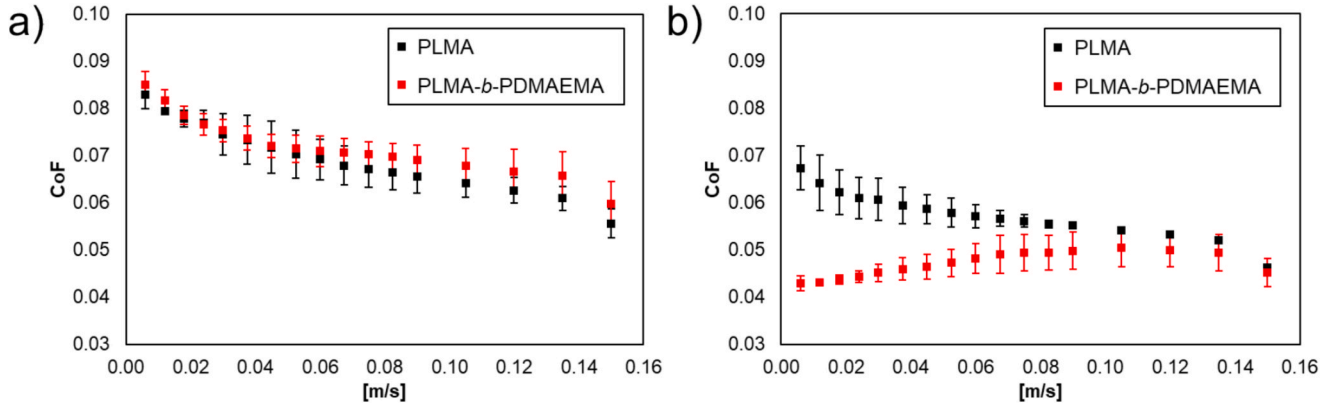

Fig. 4. Friction properties of PLMA and PLMA-*b*-PDMAEMA on Pure DLC (a) and Si-DLC (b). The curves represent representative results from one of three repeated tests. The error bars indicate the standard deviation of the coefficient of friction values measured during a 20-second interval at each sliding speed.

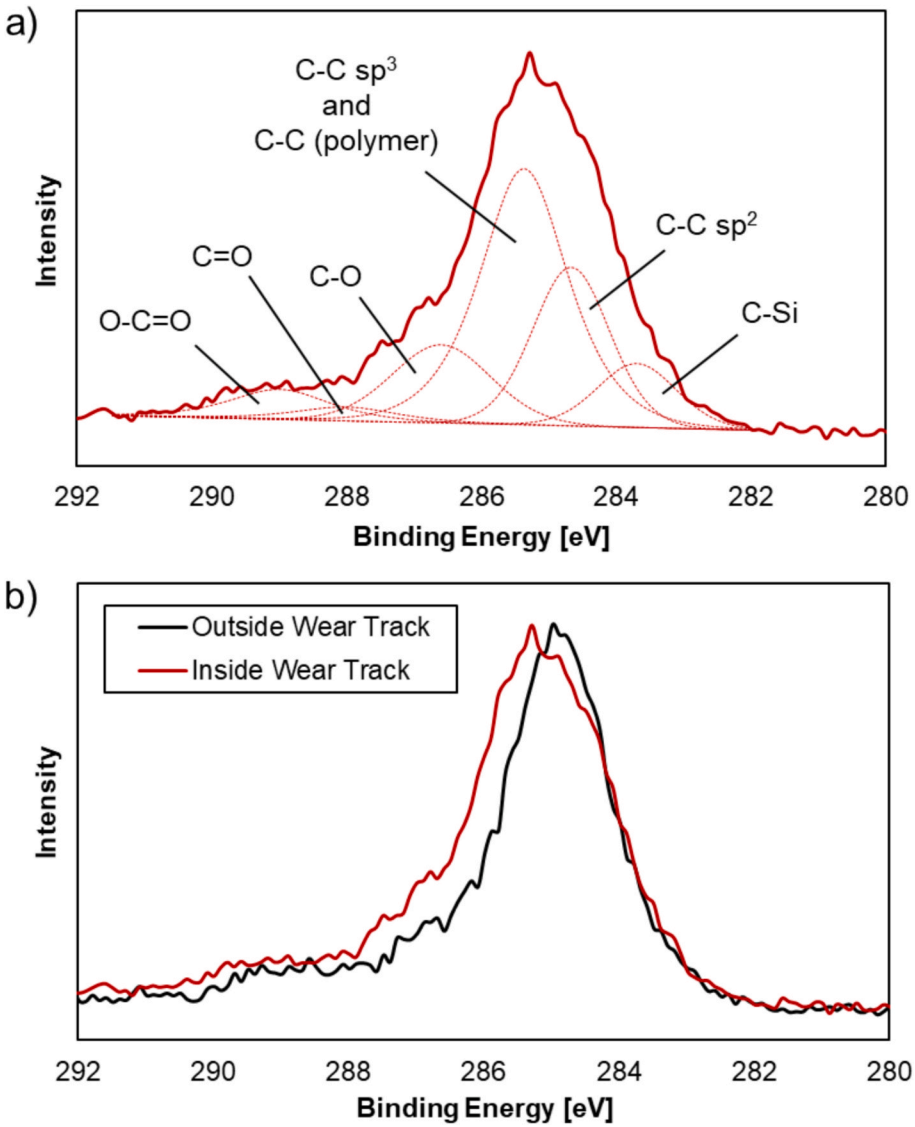

Fig. 5. High-resolution XPS carbon 1 s spectra on Si-DLC after tribology tests in the presence of PLMA-*b*-PDMAEMA. (a) Peak assignments inside the wear track. (b) Comparison of the C 1 s spectra outside (black line) and inside the wear track (red line).

adequately describe the dangling bonds of DLC surface. Ultrasoft pseudopotentials [27] were used to approximate the core electrons, using a cutoff of 40 Ry for the kinetic energy and 320 Ry for the charge density were employed. The lateral size of the undoped DLC and Si-DLC simulation cells was 18.8 Å × 15.0 Å with a slab thickness of ~ 10 Å. A vacuum region of at least 10 Å was included in the z-direction to avoid unwanted interactions with the periodic replicas, so that the height of the cell was between 24 Å (adsorption study) and 40 Å (impact MD). The Brillouin zone was only sampled at the Γ-point due to the large size of the cells.

For the sliding MD simulation, a normal load of 1 GPa was applied on the upper DLC slab, and the positions of the atoms in the lower region of the bottom Si-DLC slab were fixed to equalize the load. The atoms in the uppermost region of the upper slab were moved at a constant speed of 200 m/s in the x-direction to simulate the sliding conditions. Although such a high speed is not entirely realistic, it is a necessary compromise to observe sliding at least in the nanometer range within the time scales allowed by ab initio MD. Both slabs were kept at 80 °C (the temperature of the experiment) by a velocity-rescaling thermostat, except for the interface region, to reduce the spurious effects of the thermostat on the polymer adsorption processes. The Verlet integration algorithm with a time step of 1.45 fs was used for the evolution of the equations of motion. The sliding simulation was performed for 15 ps, while the impact simulations were interrupted at shorter times, a few picoseconds after the impact.

3. Results

3.1. Tribology test

Tribological experiments were conducted to assess the friction behavior of PLMA and PLMA-*b*-PDMAEMA on both Pure DLC and Si-DLC coatings. The friction coefficients measured at different sliding speeds are presented in Fig. 4. For the Pure DLC coating, the presence of amino functional groups in the copolymer did not lead to a significant change in friction behavior. In the Si-DLC coating, however, the tribological performance of the different polymers differed significantly, with PLMA-*b*-PDMAEMA showing a marked reduction in friction. To verify the robustness of the observed friction-reducing mechanism, additional tribological tests were performed at significantly higher loads up to 100 N using the same copolymer and Si-DLC system (**Fig. S4**). Furthermore, temperature-dependent tests were conducted at 60 °C and 80 °C to

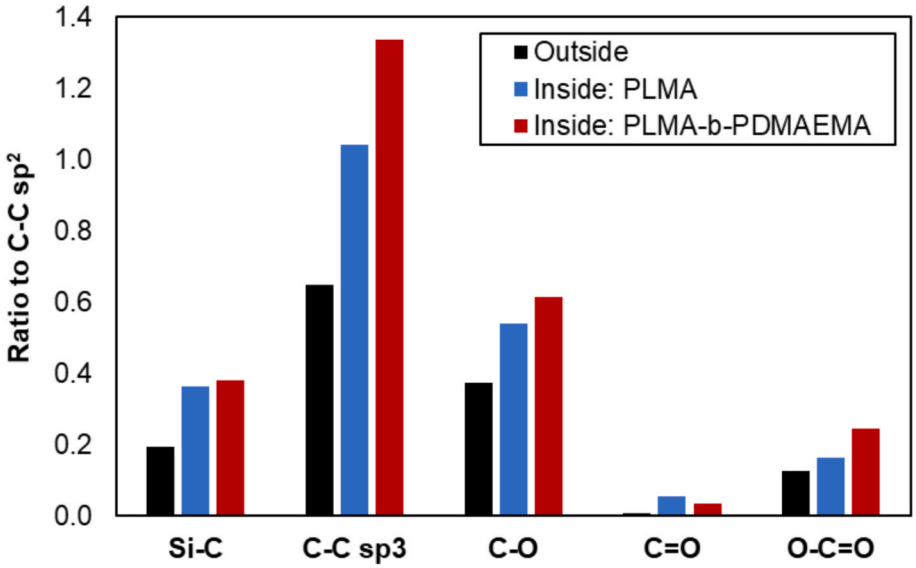

Fig. 6. Ratios of each C 1 s peak intensity normalized to the C–C sp^2 bond, obtained from the regions inside and outside the wear track in the presence of either PLMA or PLMA-*b*-PDMAEMA on Si-DLC.

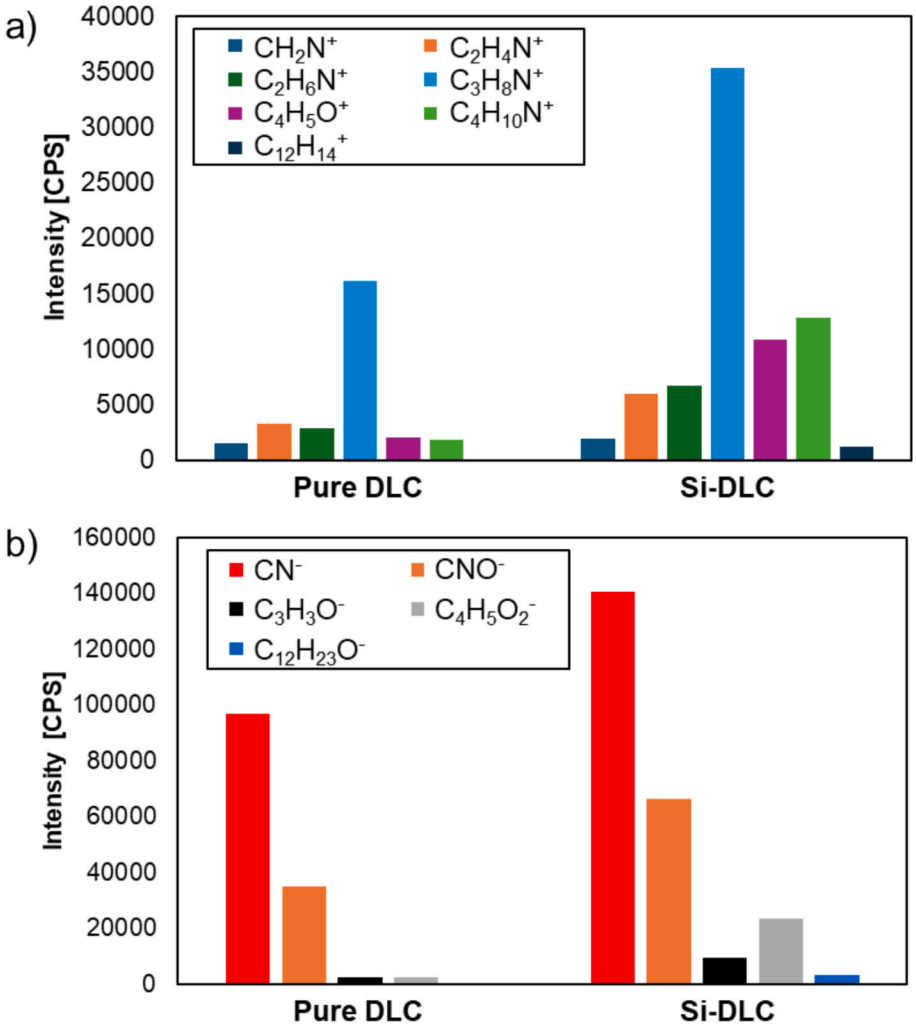

Fig. 7. (a) Positive ion fragment intensities and (b) negative ion fragment intensities obtained from wear tracks on Pure DLC and Si-DLC in the presence of PLMA-*b*-PDMAEMA.

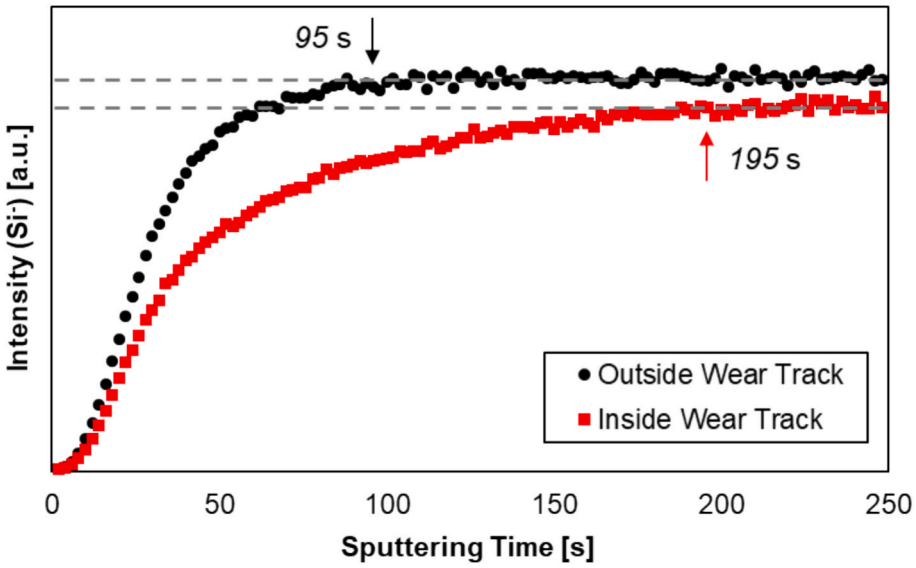

Fig. 8. ToF-SIMS depth profiles of Si^- from measurements conducted on Si-DLC samples subjected to tribological testing with PLMA-*b*-PDMAEMA. The profiles represent regions outside (black) and inside (red) the wear tracks. The grey dashed lines indicate the steady-state intensity levels for each profile, and the approximate sputtering times at which these steady-state intensities are reached are also shown.

evaluate the thermal responsiveness of the copolymer films (**Fig. S5**). These tests demonstrated that the functionalized copolymer maintained a lower coefficient of friction than the non-functionalized one at both temperatures.

3.2. Surface analysis using XPS

Ex-situ XPS was performed to analyze the chemical composition of the tribofilm on the wear tracks after the tribology tests. Fig. 5 shows the high-resolution carbon 1 s (C 1 s) spectra after the tribology test in the presence of PLMA-*b*-PDMAEMA on Si-DLC. The analysis of the C 1 s spectra attributed six peaks: C-Si bonds (283.5 ± 0.2 eV), C–C sp^2 bonds (284.6 ± 0.2 eV), C–C sp^3 bonds (285.3 ± 0.2 eV), C-O bonds (286.6 ± 0.2 eV), C=O (288.0 ± 0.2 eV), and O-C=O (288.8 ± 0.2 eV) (Fig. 5**(a)**) [28–34]. The separation of the C–C sp^2 and C–C sp^3 states was fixed at 0.7 eV. Fig. 5**(b)** shows the C 1 s spectra in the presence of PLMA-*b*-PDMAEMA on Si-DLC, where the peak intensities are normalized for comparison. The black line represents the peaks outside the wear track, while the red line represents the peaks inside the wear track. Compared to the spectra outside the wear track, the spectra on the wear track show an increase in the peaks, particularly for C–C sp^3 bonds, C-O bonds, and O-C=O bonds. The C–C sp^3 bonds are abundant not only in DLC but also in the copolymer, while C-O bonds and C=O bonds are abundant in the backbone of PLMA-*b*-PDMAEMA. The increase in the number of these bonds suggests the presence of a significant amount of copolymer on the wear track.

Additionally, a comparison of the C 1 s spectra was conducted between the regions inside and outside the wear track in the presence of PLMA or PLMA-*b*-PDMAEMA. The ratios of the peak intensities, each normalized to the C–C sp^2 bond, are shown in Fig. 6. The C–C sp^2 bond, which is present in DLC films but not in the copolymer was thus used as a reference value. The comparative results show that the wear track in the presence of PLMA-*b*-PDMAEMA has the highest value of C–C sp^3 bonds, C-O bonds, and O-C=O bonds. This indicates that the wear track in the presence of PLMA-*b*-PDMAEMA contains the most copolymer-derived carbon bonds. This suggests that DMAEMA, with an amino functional group, enhances adsorption on the Si-DLC surface, thereby promoting the formation of a tribofilm from the copolymer during the tribology test. The nitrogen content in the tribofilm after testing was estimated to be approximately 1 atomic percent, based on XPS survey scans. Due to this low concentration, the signal-to-noise ratio in the N 1 s and Si 2p regions was insufficient to allow reliable peak deconvolution for quantifying N–Si bonding.

3.3. Surface analysis using ToF-SIMS

To gain a deeper understanding of the molecular structure within the tribofilm induced by silicon dopants, surface analysis on the wear tracks was conducted using ToF-SIMS. Fig. 7 shows the comparative results of representative ToF-SIMS ion intensities on wear tracks in the presence of PLMA-*b*-PDMAEMA on Pure DLC and Si-DLC. From the positive ion fragments in Fig. 7**(a)**, CH_2N^+ (*m/z* 28), $C_2H_4N^+$ (*m/z* 42), $C_2H_6N^+$ (*m/z* 44), $C_3H_8N^+$ (*m/z* 58), $C_4H_5O^+$ (*m/z* 69), $C_4H_{10}N+$ (*m/z* 72), and $C_{12}H_{14}^+$ (*m/z* 158) were identified as positive ion signals from PDMAEMA chains [35]. Fig. 7**(b)** shows the negative ion fragment intensities, where CN^- (*m/z* 26), CNO^- (*m/z* 42), $C_3H_3O^-$ (*m/z* 55), and $C_4H_5O_2^-$ (*m/z* 85), associated with PDMAEMA chains, were similarly detected [36–39]. Additionally, at higher mass-to-charge ratios for the negative ion fragments, $C_{12}H_{23}O^-$ (*m/z* 183) was identified as a negative ion peak derived from PLMA chains [40,41].

A comparison of the positive ion fragments shows that positive ion peaks derived from PDMAEMA were detected on Si-DLC, suggesting a significant presence of PDMAEMA fragments within the tribofilm on the wear track due to silicon doping in DLC. When comparing the negative ion fragments, not only peaks corresponding to amine groups within the PDMAEMA structure frequently detected on Si-DLC, but also peaks from the polymer backbone, such as $C_3H_3O^-$ and $C_4H_5O_2^-$, were also prevalent. However, since these peaks are also present in the polymer backbone of PLMA, it remains unclear whether these peaks originated from PDMAEMA or PLMA chains. Interestingly, although the peak of the $C_{12}H_{23}O^-$ intensity was relatively low, the presence peak clearly indicates the detection of PLMA chains.

ToF-SIMS depth profiles of Si were obtained to evaluate the thickness of the film formed on the surface during sliding in the presence of PLMA-*b*-PDMAEMA (Fig. 8). Notably, the sputtering time required to reach the steady-state intensity of the Si profile was longer inside the wear tracks than outside. This result suggests that the surface was covered by a relatively thick polymer film anchored via N–Si bonds in the DLC layer, requiring more sputtering before the underlying Si-DLC is fully exposed.

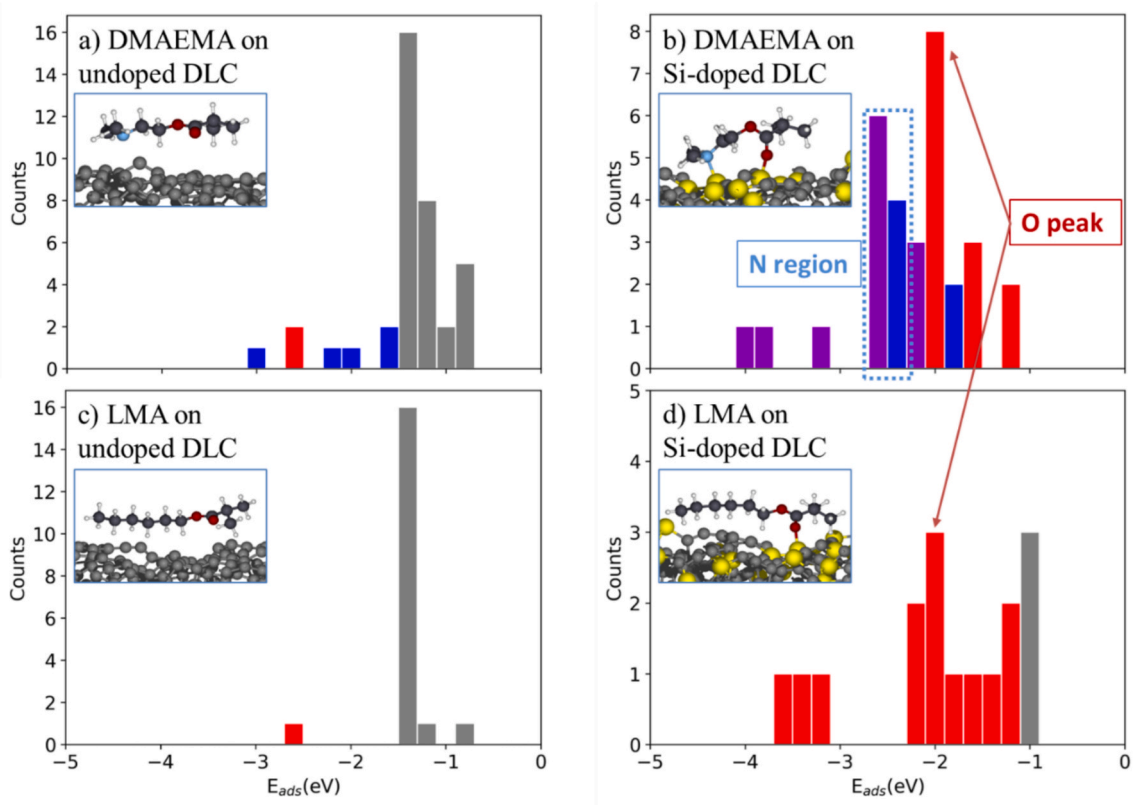

Fig. 9. Histograms of the distribution of adsorption energies for a) DMAEMA on undoped DLC, b) DMAEMA on Si-DLC, c) LMA on undoped DLC, d) LMA on Si-DLC. The color code of the bars is the following: grey for physisorption, red for chemisorption involving oxygen, blue for chemisorption involving nitrogen, and violet for chemisorption with both O and N. If more than one bonding configuration was present in the same bar, the color of the most frequent one was selected. An inset with a representative adsorption configuration is included for each molecule-surface combination.

3.4. Adsorption and dissociation calculations

Ab initio molecular adsorption calculations were performed to investigate the effect of the functional group and the Si-doping of the DLC surface on the adsorption process that can lead to the formation of a tribofilm. By using the Xsorb program, we were able to automatically generate a very large number of initial adsorption configurations (>400) for DMAEMA and LMA on undoped and Si-doped DLC, differing by the lateral position of the molecule on the surface and by the orientation (rotation) of the molecule. The program automatically selected a subset of 120 configurations by choosing the most stable one for each adsorption site among the different molecular rotations for that site. These configurations were fully optimized, and their adsorption energies are reported in Fig. 9, where a color code is used to indicate adsorption through different bonds. For each molecule-surface combination, the corresponding histogram shows the distribution of adsorption energy, defined as

$$E_{ads} = E_{slab+mol} - E_{slab} - E_{mol}$$

where $E_{slab+mol}$ is the energy of the structure with the molecule adsorbed on the slab, E_{slab} is the energy of the slab without the molecule, and E_{mol} is the energy of the molecule in vacuum. With this definition, more negative values of adsorption energy correspond to more favorable adsorption.

Fig. 9**(a,c)** clearly show that on undoped DLC both molecules are only physisorbed, with just a negligible amount of bonded configurations due the high reactivity of some highly under-coordinated carbon atoms on the surface. The adsorption energy distributions for the two molecules show identical dominant peak at −1.4 eV, which contains almost all occurrences for LMA, while DMAEMA shows a larger variance, being mildly more reactive also on undoped DLC due to the presence of nitrogen. On Si-doped DLC the picture changes completely as can be seen, in Fig. 9**(b,d)**, where both molecules increased reactivity. For DMAEMA, all configurations are chemisorbed, with one or more bonds formed of, either N-Si, O-Si or both simultaneously, as visible in the inset of Fig. 9**b**. A peak at −2 eV is related with chemisorption by oxygen, while the region between [-2.6 eV, −2.4 eV] is mainly associated with chemisorption by nitrogen, with a few cases where both nitrogen and oxygen are bonded to Si atoms. Some very favorable adsorption configurations were found around −4 eV, strongly bound by

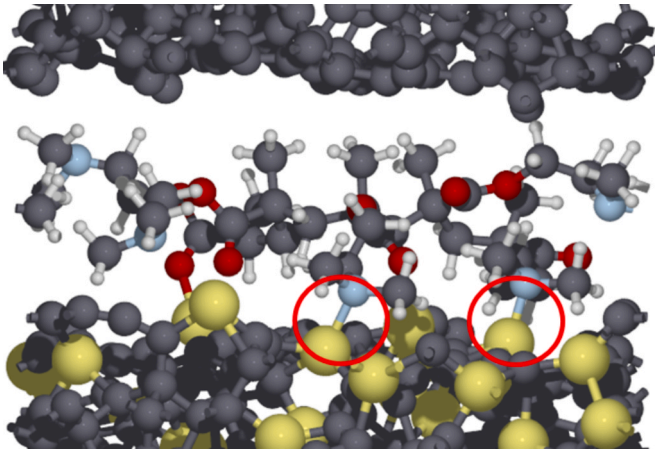

Fig. 10. Final structure of the 5-DMAEMA polymer at the end of a 15 ps sliding AIMD on Si-DLC at 1 GPa load. Two N-Si bonds, circled in red, are spontaneously formed at the beginning of the simulation, and remain stable for the whole time. An O-Si bond is also formed.

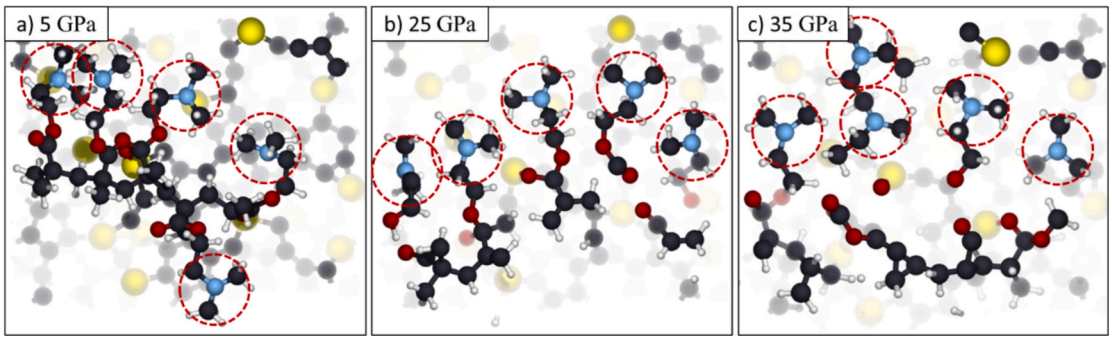

Fig. 11. 5-DMAEMA polymer after the impact for peak pressure of 5GPa (a), 25 GPa (b) and 35 GPa (c). At 5 GPa the polymer is completely unaffected, and no dissociation occurred. At much higher pressures, even if a few C-O and C–C bond breaking are present, none of the N-C_3 functional units (circled in red) dissociates.

both N-Si and O-Si. Improved reactivity was observed also for LMA compared to undoped DLC, with the same oxygen peak at −2 eV as for DMAEMA. However, in contrast to DMAEMA, physisorbed-only configurations are present, and excluding the few outliers at very low energy and the oxygen peak at −2 eV (present in both), LMA has no bonds in the "N region" between [-2.6 eV, −2.4 eV], which is instead highly populated for DMAEMA due to N-Si bonds. Moreover, as explained in our previous study, the oxygen bonds are less relevant for LMA because the oxygen atoms in the real copolymer are close to the polymer backbone, and the hydrocarbon chains are twice as long as this adsorption study, so it is very likely that the oxygen atoms can only rarely come into contact with the Si-DLC surface due to steric hindrance from the hydrocarbon chains. In DMAEMA, however, the N atoms are located at the end of the monomers, which means that they can easily reach the surface.

Having established that DMAEMA forms very strong N-Si bonds on Si-DLC, the stability of DMAEMA chemisorption in tribological conditions of sliding under load was tested with an AIMD simulation for a small 5-DMAEMA polymer under 1 GPa of applied load, at a temperature of 80 °C, mimicking the experimental conditions.

As visible in Fig. 10, DMAEMA spontaneously chemisorbed, forming two N-Si bonds and an O-Si bond, which did not break during sliding. This confirms that DMAEMA can remain stably anchored to the Si-DLC substrate even during sliding in tribological conditions.

Finally, the mechanically activated dissociation patterns of the functional groups of the copolymer were studied to find out whether tribochemical reactions play an important role in the tribofilm formation, or the film is simply formed by adsorbed copolymers (anchored through the chemisorbed functional groups) and the friction reduction/load carrying capacity are given by the viscoelasticity and steric hindrance of LMA hydrocarbon tails that constitute most of the copolymer. To obtain an indication of the copolymer's tendency to dissociate, we performed "impact" molecular dynamics simulations, in which a 5-DMAEMA functional polymer was placed within a Si-DLC – undoped DLC interface and the top slab was accelerated downwards by the application of an external normal force. This acceleration ultimately leads to an impulsive collision where the mechanical stress on the polymer is much higher than the nominal load, mimicking the extremely high local stresses that can occur at the contact between surface asperities. Three impact simulations were conducted for increasing values of peak impact pressure, reaching approximately 5GPa, 25GPa and 35GPa, respectively. While local pressures spikes above 15–20 GPa (hardness limit of Si-DLC) are not likely to be reached in real experimental conditions, they can be considered as a limit case to investigate the possibility of mechanically-induced dissociations of dimethylamino groups within the limited statistics allowed by the small time and spatial scales of ab initio simulations.

The status of the 5-DMAEMA polymer after the collision for the different pressures is reported in Fig. 11.

For 5 GPa of peak pressure, no dissociation of the polymer took place,

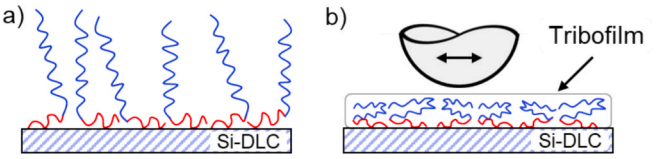

Fig. 12. Two-step mechanism of tribofilm formation: (a) Chemical adsorption process of the functionalized copolymer onto the Si-DLC surface and (b) schematic representation of the compression of the functionalized copolymer during the tribological test. In both panels, the blue segments represent the lipophilic PLMA block, and the red segments represent the amino-functional PDMAEMA block. The PDMAEMA segments anchor to the Si-DLC surface via chemisorption, promoting the formation of a tribofilm under mechanical compression.

which means that the inter-molecular bonds are very resistant to mechanical stress. At 25 GPa of peak pressure some bond breaking occurred, mainly in the polymer backbone, separating the monomers, and a few C-O bonds were also broken, but no bond breaking is observed for the N-C bonds in the N-C_3 functional units. At 35 GPa, more fragmentation occurred, but even under such extreme conditions (never reached in the real experiments) no C-N bond breaking was observed, meaning that the dimethylamino group is extremely stable, and therefore it is very unlikely that the lubricating film is the result of C-N bond dissociation and the formation of a new material from tribochemical reactions, like the tribofilm formed by other additives such as ZDDP [42].

In summary, the experimental surface analysis and the computational results show that the Si-doping of DLC is crucial for the adsorption of the copolymer, and they strongly suggest that the short DMAEMA chains, with nitrogen end groups, act as very stable anchoring points for the whole copolymer, while the LMA units act as an interfacial film that reduces friction due to viscoelasticity and prevents surface-to-surface contact by steric hindrance of the inert hydrocarbon chains. A schematic representation of the adsorption process and the tribological processes involved in tribofilm formation can be seen in Fig. 12. In the figure, the blue segments represent the PLMA block, which forms the outer layer of the copolymer and contributes to the oleophilic. The red segments represent the PDMAEMA block, which contains nitrogen functional groups responsible for anchoring to the Si-DLC surface via chemical adsorption.

First, the amine groups in the PDMAEMA units of PLMA-*b*-PDMAEMA actively adsorb to the silicon dopants on the Si-DLC surface. This process forms a lubricating film that exhibits friction-reducing properties. During tribological tests conducted, the adsorbed polymer undergoes compression over time, leading to the formation of a tribofilm. Unlike other additives such as ZDDP, the film formation mechanism does not involve tribochemical reaction of decomposition and recombination of the functional groups, which are shown to be extremely stable by the dissociation analysis. Instead, the adsorbed

Funded by the European Union

polymer remains intact and is compressed into a stable tribofilm which contributes to friction reduction.

4. Conclusion

This study has successfully elucidated the tribological mechanisms underlying the interaction between functionalized copolymers and Si-DLC coatings. The experimental results from tribological tests, combined with surface analyses by XPS and ToF-SIMS and supported by ab initio simulations, revealed a two-step mechanism for tribofilm formation. The first step involves the chemical adsorption of the functionalized copolymer, specifically PLMA-b-PDMAEMA, onto the Si-DLC surface via its terminal amine groups, which is facilitated by the formation of strong N-Si bonds. This adsorption process creates a stable lubricating film that reduces friction. The second step occurs in tribological tests, where the adsorbed polymer undergoes compression, forming a durable tribofilm without significant chemical decomposition or tribochemical reactions, typically observed with additives like ZDDP.

The study highlights the importance of Si doping in DLC coatings to improve the adsorption and stability of functionalized copolymers, particularly those containing DMAEMA groups. The stability of the polymer under both sliding and impact conditions underlines its suitability as a boundary lubricant. The LMA units contribute to friction reduction through viscoelasticity and steric hindrance and complements the anchoring function of the DMAEMA units. Taken together, these results provide valuable insights into the development of advanced lubrication systems. They show how the synergy between functionalized copolymers and doped DLC coatings can lead to superior friction reduction and wear resistance, paving the way for the development of high-performance, sustainable lubrication solutions.

CRediT authorship contribution statement

Takeru Omiya: Writing – original draft, Visualization, Validation, Software, Methodology, Investigation, Formal analysis, Data curation, Conceptualization. **Enrico Pedretti:** Writing – original draft, Visualization, Validation, Software, Methodology, Investigation, Formal analysis, Data curation. **Albano Cavaleiro:** Writing – review & editing, Supervision, Resources, Project administration, Funding acquisition. **Rachel Gouttebaron:** Writing – review & editing, Methodology, Formal analysis, Data curation. **Alexandre Felten:** Writing – review & editing, Software, Methodology, Formal analysis, Data curation. **Arménio C. Serra:** Writing – review & editing, Resources, Funding acquisition. **Jorge F.J. Coelho:** Writing – review & editing, Supervision, Resources, Project administration, Funding acquisition, Conceptualization. **Maria Clelia Righi:** Writing – review & editing, Supervision, Resources, Project administration, Investigation, Funding acquisition, Conceptualization. **Fábio Ferreira:** Writing – review & editing, Supervision, Resources, Project administration, Funding acquisition, Conceptualization.

Declaration of competing interest

The authors declare that they have no known competing financial interests or personal relationships that could have appeared to influence the work reported in this paper.

Acknowledgments

This research is sponsored by national funds through FCT – Fundação para a Ciência e a Tecnologia, under the project UIDB/00285/2020, LA/P/0112/2020, 2023.08138.CEECIND/CP2832/CT0005, SmartHyLub (2022.05603.PTDC), iLub (2022.15609.UTA), UniLub (2023.17357.ICDT) and by the Taiho Kogyo Tribology Research Foundation (Grant No. 22A25). This project has received funding from the European Union's Horizon 2020 research and innovation programme under grant agreement No 101007417, having benefited from the access provided by the University of Namur in Namur Institute of Structured Matter within the framework of the NFFA-Europe Pilot Transnational Access Activity, proposal ID505.

These results are part of the "Advancing Solid Interface and Lubricants by First Principles Material Design (SLIDE)" project that has received funding from the European Research Council (ERC) under the European Union's Horizon 2020 research and innovation program (Grant agreement No. 865633).

Appendix A. Supplementary data

Supplementary data to this article can be found online at https://doi.org/10.1016/j.apsusc.2025.163599.

Data availability

Data will be made available on request.

References

[1] A. Boehm, Lubricating-oil improvers, in: Proc. API Annual Meeting, 1948, pp. 35-41.
[2] E. Okrent, The effect of lubricant viscosity and composition on engine friction and bearing wear, ASLE TRANSACTIONS 4 (1961) 97–108.
[3] P. Cann, H. Spikes, The behavior of polymer solutions in concentrated contacts: immobile surface layer formation, Tribol. Trans. 37 (1994) 580–586.
[4] S. Gunsel, M. Smeeth, H. Spikes, Friction and wear reduction by boundary film-forming viscosity index improvers, SAE Trans. (1996) 1831–1855.
[5] M. Smeeth, H. Spikes, S. Gunsel, Boundary film formation by viscosity index improvers, Tribol. Trans. 39 (1996) 726–734.
[6] M. Smeeth, H. Spikes, S. Gunsel, The formation of viscous surface films by polymer solutions: boundary or elastohydrodynamic lubrication? Tribol. Trans. 39 (1996) 720–725.
[7] M. Muller, K. Topolovec-Miklozic, A. Dardin, H.A. Spikes, The design of boundary film-forming PMA viscosity modifiers, Tribol. Trans. 49 (2006) 225–232.
[8] J. Cayer-Barrioz, D. Mazuyer, A. Tonck, E. Yamaguchi, Frictional rheology of a confined adsorbed polymer layer, Langmuir 25 (2009) 10802–10810.
[9] R.M. Bielecki, M. Crobu, N.D. Spencer, Polymer-brush lubrication in oil: sliding beyond the stribeck curve, Tribol. Lett. 49 (2013) 263–272.
[10] T. Omiya, F. De Bon, T. Vuchkov, A. Serra, A. Cavaleiro, J. Coelho, F. Ferreira, Wear resistance by copolymers with controlled structure under boundary lubrication conditions, Lubr. Sci. 36 (2024) 1–8.
[11] J. Fan, M. Müller, T. Stöhr, H.A. Spikes, Reduction of Friction by Functionalised Viscosity Index Improvers, Tribol. Lett. 28 (2007) 287–298.
[12] T.A. Gmür, J. Mandal, J. Cayer-Barrioz, N.D. Spencer, Towards a Polymer-Brush-Based friction modifier for oil, Tribol. Lett. 69 (2021) 124.
[13] S. Delamarre, T. Gmür, N.D. Spencer, J. Cayer-Barrioz, Polymeric friction modifiers: Influence of anchoring chemistry on their adsorption and effectiveness, Langmuir, 38 (2022) 11451-11458.
[14] M. Kano, Y. Yasuda, Y. Okamoto, Y. Mabuchi, T. Hamada, T. Ueno, J. Ye, S. Konishi, S. Takeshima, J. Martin, Ultralow friction of DLC in presence of glycerol mono-oleate (GNO), Tribol. Lett. 18 (2005) 245–251.
[15] C. Matta, L. Joly-Pottuz, M. De Barros Bouchet, J. Martin, M. Kano, Q. Zhang, W., Goddard III, Superlubricity and tribochemistry of polyhydric alcohols, Physical Review B—Condensed Matter and Materials, Physics 78 (2008) 085436.

[16] S. Yi, X. Chen, J. Li, Y. Liu, S. Ding, J. Luo, Macroscale superlubricity of Si-doped diamond-like carbon film enabled by graphene oxide as additives, Carbon 176 (2021) 358–366.
[17] S. Yi, J. Li, J. Rao, X. Ma, Y. Zhang, Alkyl-functionalized black phosphorus nanosheets triggers macroscale superlubricity on diamond-like carbon film, Chem. Eng. J. 449 (2022) 137764.
[18] T. Omiya, E. Pedretti, M. Evaristo, A. Cavaleiro, A.C. Serra, J.F. Coelho, F. Ferreira, M.C. Righi, Synergistic effects of nitrogen-containing functionalized copolymer and silicon-doped DLC for friction and wear reduction, Tribol. Int. 200 (2024) 110183.
[19] M. Evaristo, R. Azevedo, C. Palacio, A. Cavaleiro, Influence of the silicon and oxygen content on the properties of non-hydrogenated amorphous carbon coatings, Diam. Relat. Mater. 70 (2016) 201–210.
[20] B.J. Hamrock, D. Dowson, Ball Bearing Lubrication (The Elastohydrodynamics of Elliptical Contacts), J. Lubr. Technol. 104 (1981) 279–281.
[21] P. Hohenberg, W. Kohn, Inhomogeneous electron gas, Phys. Rev. 136 (1964) B864.
[22] B. Deng, P. Zhong, K. Jun, J. Riebesell, K. Han, C.J. Bartel, G. Ceder, CHGNet as a pretrained universal neural network potential for charge-informed atomistic modelling, Nat. Mach. Intell. 5 (2023) 1031–1041.
[23] E. Pedretti, P. Restuccia, M.C. Righi, Xsorb: a software for identifying the most stable adsorption configuration and energy of a molecule on a crystal surface, Comput. Phys. Commun. 291 (2023) 108827.
[24] P. Giannozzi, S. Baroni, N. Bonini, M. Calandra, R. Car, C. Cavazzoni, D. Ceresoli, G.L. Chiarotti, M. Cococcioni, I. Dabo, QUANTUM ESPRESSO: a modular and open-source software project for quantum simulations of materials, J. Phys. Condens. Matter 21 (2009) 395502.
[25] J.P. Perdew, K. Burke, M. Ernzerhof, Generalized gradient approximation made simple, Phys. Rev. Lett. 77 (1996) 3865.
[26] S. Grimme, Semiempirical GGA-type density functional constructed with a long-range dispersion correction, J. Comput. Chem. 27 (2006) 1787–1799.
[27] D. Vanderbilt, Soft self-consistent pseudopotentials in a generalized eigenvalue formalism, Phys. Rev. B 41 (1990) 7892.
[28] G.D. Sorarù, G. D'Andrea, A. Glisenti, XPS characterization of gel-derived silicon oxycarbide glasses, Mater. Lett. 27 (1996) 1–5.
[29] Y. Hijikata, H. Yaguchi, M. Yoshikawa, S. Yoshida, Composition analysis of SiO2/SiC interfaces by electron spectroscopic measurements using slope-shaped oxide films, Appl. Surf. Sci. 184 (2001) 161–166.
[30] X. Yan, T. Xu, S. Yang, H. Liu, Q. Xue, Characterization of hydrogenated diamond-like carbon films electrochemically deposited on a silicon substrate, J. Phys. D Appl. Phys. 37 (2004) 2416.
[31] G. Wan, P. Yang, R.K. Fu, Y. Mei, T. Qiu, S. Kwok, J.P. Ho, N. Huang, X. Wu, P. K. Chu, Characteristics and surface energy of silicon-doped diamond-like carbon films fabricated by plasma immersion ion implantation and deposition, Diam. Relat. Mater. 15 (2006) 1276–1281.
[32] A. Bendavid, P. Martin, C. Comte, E. Preston, A. Haq, F.M. Ismail, R. Singh, The mechanical and biocompatibility properties of DLC-Si films prepared by pulsed DC plasma activated chemical vapor deposition, Diam. Relat. Mater. 16 (2007) 1616–1622.
[33] M.H. Ahmed, J.A. Byrne, J. McLaughlin, W. Ahmed, Study of human serum albumin adsorption and conformational change on DLC and silicon doped DLC using XPS and FTIR spectroscopy, (2013).
[34] Y.L. Khung, S.H. Ngalim, A. Scaccabarozzi, D. Narducci, Formation of stable Si–O–C submonolayers on hydrogen-terminated silicon (111) under low-temperature conditions, Beilstein J. Nanotechnol. 6 (2015) 19–26.
[35] M. Tohyama, T. Ohmori, A. Murase, M. Masuko, Friction reducing effect of multiply adsorptive organic polymer, Tribol. Int. 42 (2009) 926–933.
[36] P. Lazzeri, L. Vanzetti, M. Anderle, M. Bersani, J. Park, Z. Lin, R. Briber, G. Rubloff, H. Kim, R. Miller, Thin-film transformations and volatile products in the formation of nanoporous low-k polymethylsilsesquioxane-based dielectric, Journal of Vacuum Science & Technology B: Microelectronics and Nanometer Structures Processing, Measurement, and Phenomena 23 (2005) 908–917.
[37] Q. Peng, D.M. Lai, E. Kang, K. Neoh, Preparation of polymer-silicon (100) hybrids via interface-initiated reversible addition-fragmentation chain-transfer (RAFT) polymerization, (2006).
[38] P. Teper, J. Chojniak-Gronek, A. Hercog, N. Oleszko-Torbus, G. Płaza, J. Kubacki, K. Balin, A. Kowalczuk, B. Mendrek, Nanolayers of poly (N, N′-Dimethylaminoethyl methacrylate) with a star topology and their antibacterial activity, Polymers 12 (2020) 230.
[39] M. Flejszar, K. Ślusarczyk, A. Hochół, P. Chmielarz, M. Wytrwal, K. Wolski, K. Spilarewicz, K. Awsiuk, J. Raczkowska, Sequential SI-ATRP in μL-scale for surface nanoengineering: A new concept for designing polyelectrolyte nanolayers formed by complex architecture polymers, Eur. Polym. J. 194 (2023) 112142.
[40] D. Briggs, A. Brown, J.C. Vickerman, F. Adams, Handbook of static secondary ion mass spectrometry (SIMS), Anal. Chim. Acta 236 (1990) 509–510.
[41] S. Clarke, M.C. Davies, C.J. Roberts, S.J. Tendler, P.M. Williams, V. O'Byrne, A. L. Lewis, J. Russell, Surface mobility of 2-methacryloyloxyethyl phosphorylcholine-co-lauryl methacrylate polymers, Langmuir 16 (2000) 5116–5122.
[42] R. Mourhatch, P.B. Aswath, Tribological behavior and nature of tribofilms generated from fluorinated ZDDP in comparison to ZDDP under extreme pressure conditions—Part II: Morphology and nanoscale properties of tribofilms, Tribol. Int. 44 (2011) 201–210.